Progress In Electromagnetics Research C, Vol. 42, 1–11, 2013

CHARACTERIZATION OF LOSSY SIW RESONATORS BASED ON MULTILAYER PERCEPTRON NEURAL NETWORKS ON GRAPHICS PROCESSING UNIT

Giandomenico Amendola[1], Giovanni Angiulli[2, *], Emilio Arnieri[1], Luigi Boccia[1], and Domenico De Carlo[2]

[1]DEIS, Univ. della Calabria, via Pietro Bucci, Rende (CS) 87036, Italy

[2]DIIES, Univ. Mediterranea, via Graziella, Loc. Feo di Vito, Reggio Calabria 89121, Italy

Abstract—In recent years, Artificial Neural networks (ANNs) have been intensively employed to build smart model of microwave devices. In this paper a characterization of lossy SIW resonators by means of Multilayer Perceptron Neural Networks (MLPNNs) on Graphics Processing Unit (GPU), is presented. Once properly selected and trained, a MLPNN can evaluate the lossy SIW resonator's resonant frequency f_r and the pertaining quality factor Q at a shorter time than the full-wave rigorous model. In this way, fast parametric models of SIW structures to employ for the design and optimization of microwave devices, exploiting the computational power of GPUs, can be obtained.

1. INTRODUCTION

Substrate integrated waveguides is nowadays a recognized field of research. All kind of devices, operating in the regions of microwaves and millimeter waves, have been developed making SIW a well established technology. Filters [1], antennas [2], power combiners [3, 4] and other devices have been successfully designed and realized. The design of such devices can be faced with the help of commercial codes based on finite methods like FEM [5], however, in a series of papers [6–9] the authors have shown alternative and more effective methods to analyze SIW structures. In particular the method based on the dyadic Green's function technique and the method of moments proved to be effective and accurate and it has been applied to the analysis of both non radiating [7] and radiating [8] structures and, recently, has

Received 10 May 2013, Accepted 9 July 2013, Scheduled 15 July 2013

* Corresponding author: Giovanni Angiulli (giovanni.angiulli@unirc.it).

been extended to lossy SIW devices [9]. The method provided also an easy way to analyze SIW resonators. In [10, 11, 23] the characteristics of SIW cavity have been proposed but losses were not taken into account and no results on quality factor were given. In [12] losses on the top and bottom plates and in the dielectric are included and results on quality factor are also given. It is well known that to improve the performances of the computer-aided design techniques to design complex microwave devices and circuits the development of smart models is essential ([13] and references within). As far as SIW structures are concerned, in [14] a support regression machine was implemented to evaluate the resonant frequencies of lossless SIW resonators. In this paper, in order to develop an efficient tool for the design and the optimization of lossy SIW resonator, a characterization using a computational intelligence approach by means of Multilayer Perceptron Neural Networks (MLPNN) on GPU, has been chosen. The implementation of a support vector machine for the lossy case and its comparison with the MLPNN will be the subject of a future work. In the last years Artificial Neural Networks (ANNs) have been recognized as useful alternative to conventional approaches usually exploited in CAD models (see [15, 16] and references within). Now, due to the nature of the ANNs' algorithms, the performances of these models can be enhanced exploiting both highly parallel architecture and processing power of Graphics Processing Units (GPUs) (see [17, 18] and references within). The paper is organized as follows: Section 2 gives a brief description of the method used to model lossy SIW resonators, together the algorithm to compute their complex resonance frequency f_r and related quality factor Q. Sections 3 and 4 give as short account on MLPNN and GPUs. Numerical results relevant to MLPNN models of lossy SIW resonators are given in Section 5. Finally, in Section 6, we draw our conclusions.

2. RESONANCES AND QUALITY FACTOR Q OF LOSSY SIW RESONATORS

The detailed study of a lossy parallel plates waveguide using the rigorous derivation of the dyadic Green's function, has been presented in [9]. Here we recall only the main ideas and results regarding the analysis and evaluation of the resonances f_r and of the quality factor Q for SIW resonators. In a lossy SIW structure, the field into the cavity is determined using the following impedance boundary condition on the top and bottom plates and on the cylinders surface [9]

$$\hat{\rho} \times \nabla \times \mathbf{H} = -j\omega\epsilon_r\epsilon_0 \left((1+j)\sqrt{\frac{\omega\mu_0}{2\sigma}} \right) \mathbf{H} \tag{1}$$

The scattered field is expressed as a series of outgoing vector wave functions having coefficients $A^{TM}_{m,n,l}\,(A^{TE}_{m,n,l})$ computed by solving the following matrix system [7, 9]

$$\mathcal{L}^{TM,TE}\bar{A}^{TM,TE} = \bar{\Gamma}^{TM,TE} \tag{2}$$

arising from the discretization via Method of Moments of the relevant scattering operator [9]. Resonances are the frequencies for which (2) has a nontrivial solution for $\bar{\Gamma}^{TM,TE} = 0$, i.e., [23]

$$\det\left(\mathcal{L}^{TM,TE}\right) = 0 \tag{3}$$

An efficient computational method to locate resonances has been presented in [19] and is based on an estimation of the minimum singular value $\sigma_{\min}$ of the discretized operator $\mathcal{L}^{TM,TE}$ in the relevant frequency band of interest rather than the direct calculation of the determinant function (3). The algorithm, described in [19], firstly finds the behavior of $\sigma_{\min}(f_{re})$ of the matrix operator $\mathcal{L}^{TM,TE}$ as a function of the real frequency only, locating its minima on this axis. Once that this minimum is located, it is exploited as starting point of a Muller search routine in the complex plane. The final results of this procedure is the complex resonant frequency $f_{re} + jf_{im}$ of the structure at hand [10, 23]. The quality factor Q of the lossy resonator is easily computed as [12]

$$Q = \frac{f_{re}}{2f_{im}} \tag{4}$$

Because of SIW resonators are realized on substrates which are thin with respect to the wavelength only the first $TM\,to\,z$ mode is present. Accordingly, in this paper only this mode will be considered.

3. FEED FORWARD MULTILAYER PERCEPTRON NEURAL NETWORKS

Soft-computing via Artificial Neural Networks (ANNs) is an active field of research, and there exists a large literature on the topic (see [21] and references within). Briefly speaking, an ANN is a nonlinear statistical data modeling tool that changes its structure on the basis of external or internal information that flows through itself during the learning phase. Typically ANNs consist of a set of nodes, named neurons, interconnected by groups organized in input, output and hidden layers, respectively. The characteristics and performances of an ANN depend on its topology, that is, on the pattern of connections between the neurons and by the flow of propagation of data through it. In this work the feed forward multilayered perceptron neural network (MLPNN), has been used. A MLPNN can be modeled as [21]

$$\mathbf{y} = \mathbf{y}\left(\mathbf{x}, \mathbf{W}\right) \tag{5}$$

where $\mathbf{x}$ is the *input data vector*, $\mathbf{y}$ the *output responses vector*, and $\mathbf{W}$ the *weight matrix* pertaining to the network. A MLPNN works properly when for some set of inputs $\{\mathbf{x}\}$, it produces the desired set of outputs $\{\mathbf{y}\}$. This means that the weights $w_{ij} \in \mathbf{W}$ have to be suitably chosen. This task is accomplished during the supervised learning phase, or training phase T_p. Given a set of training samples $\{\hat{\mathbf{x}}_p, \hat{\mathbf{y}}_p\}$, $p \in T_p$, the elements of $\mathbf{W}$ are changed until a suitable cost function $E(\mathbf{W})$

$$E(\mathbf{W}) = \sum_{p \in T_p} E_p(\mathbf{W}) \tag{6}$$

results minimized. In (6) the term $E_p(\mathbf{W})$ is the least square error associated to the pth tuple belonging to T_p, i.e.,

$$E_p(\mathbf{W}) = \left[\frac{1}{2} \sum_{k=1}^{M} (\hat{y}_{pk} - \mathbf{y}_k(\mathbf{W}, \hat{\mathbf{x}}_p))^2 \right]^{\frac{1}{2}} \tag{7}$$

where $\mathbf{y}_k(\mathbf{W}, \hat{\mathbf{x}}_p)$ is the kth output of MLPNN corresponding to the input $\hat{\mathbf{x}}_p$ and $\hat{y}_{pk}$ is the kth element of the output vector $\hat{\mathbf{y}}_p$ (for major details see [21]). Equation (6) is a nonlinear least square optimization problem, which can be solved using several different approaches. It can be demonstrated that all the optimization algorithms exploited to this aim, are based on the following *update rule*

$$\mathbf{W}(t) = \mathbf{W}(t-1) + \Delta\mathbf{W}(t-1) \tag{8}$$

where $\Delta\mathbf{W}(t-1)$ is the updating matrix computed at the step $t-1$ of the iteration process (for an overview of the most common optimization methods employed to train MLPNNs see [21]).

4. GRAPHICS PROCESSING UNIT DEVICES

It is well known as the main computational effort to build an ANN is related to its training phase, which grows with the growth of the nodes and layers of the network. However, this task is typically amenable to be parallelized, and at this purpose, in the recent years a number of papers have been devoted to its implementation on Graphic Processing Units (GPUs) (see [17, 18] and references within). GPUs are hardware devices originally designed to perform intensive, highly parallel real time 3D graphics computations [22]. Progressively GPUs have become general computing platforms, realizing nowadays which is known as the general purpose computing on graphics processing units (GPGPU) [22]. The GPUs' huge computing performances are due to their massive parallelism capability. In fact, a GPU consists

of an array of streaming multiprocessors. Basically, a streaming multiprocessor is built up of a set of special function unit and a number of streaming processors cores or CUDA cores. Since this architecture embeds also multi-threading and scheduling functionality in hardware, thousands of threads run on hundreds of cores very efficiently, in a scalable and transparent way. By means of the Compute Unified Device Architecture (CUDA) developed by NVIDIA© [22], a software platform with a new powerful API, which extends the C/C++ language with a scalable parallel programming model, programmers have a simple and efficient tool to leverage the massively parallel resources on the GPU, which allows to implement in relative easy way routines called *kernels*. Roughly speaking, a kernel is launched on the GPU using many parallel copies of it, called *blocks* split into *threads*, which are the smallest units of parallelization for each block. This permits the partition of the task described by kernel into sub-tasks, which can be solved concurrently by independent blocks of threads, and into smaller pieces that can be computed in parallel by each thread [22]. The implementation of ANNs on GPU is usually carried out by the following steps: *i*) arranging and transfer the training data from CPU to GPU, *ii*) running of the kernels devoted to ANN training phase *ii*) transfer of the ANN estimated data from GPU to CPU (for more details see [17] and references within). For a fast prototyping of ANNs on GPUs, MATLAB© framework in conjunction with Jacket©, can be used [20]. In this way a notable simplifying in programming it is obtained. If fact Jacket© thanks to its "compile on-the-fly system" allows GPU functions to run in MATLAB's interpretive style, enabling m-files to run on GPUs without the need of rewriting them to CUDA language [20].

5. NUMERICAL RESULTS

Figure 1 shows the layout of the SIW resonators taken in consideration in this work. Since the feeding techniques normally used in the applications of these devices do not excite the TE to $\hat{z}$ mode [10], only TM modes have been considered. Two sets of MLPNN networks, one for the circular geometry and the other one for the rectangular one, have been implemented in a MATLAB code. The via hole radius a_0, the pitch p, the substrate thickness h, the dielectric constant ϵ_r, the dielectric loss tangent $\tan(\delta)$, the metal conductivity σ_m and the geometrical dimensions of the structure at hand (the length L and the width W for the rectangular case, the radius R for the circular case) were used as input parameters while the resonant frequency f_r of the fundamental mode TM_{101} and the quality factor Q were the output.

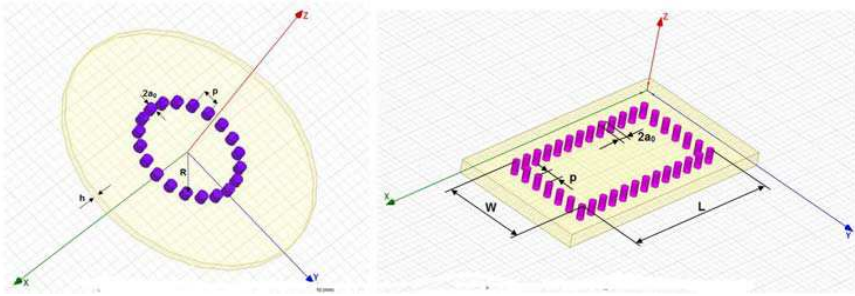

Figure 1. Circular and rectangular lossy SIW resonators, where, in particular, the pitch p, the via-hole diameter $2a_0$, the dielectric substrate height h, the sides W and L, the radius R are shown.

Table 1. Ranges of the physical parameters for the SIW resonators considered in this study (all dimensions are in millimeters, σ_m is in Siemens/meter).

a_0	p	h	ϵ_r	$\tan(\delta)$
$0.05 \div 0.8$	$0.1 \div 3.5$	$0.45 \div 0.55$	$2 \div 10$	$1.1 \cdot 10^{-3} \div 3.5 \cdot 10^{-3}$
σ_m	R	L	W	
$4.8 \cdot 10^7 \div 5.8 \cdot 10^7$	$2 \div 9.5$	$10 \div 30$	$\frac{1}{2}L$	

The ranges of variation exploited for the inputs are reported in Table 1.

Numerical simulations have been performed on an Intel Xeon DP E5405 Quad Core 2.0 GHz based workstation, with 20GB of main memory and equipped with a NVIDIA© Tesla GPU C2070 (448 streaming processor cores, 6 GB of memory). Three set of data, one of training and the others of validation and testing, having 1650, 412, and 85 tuples, respectively, were created by full wave simulations. The time required to generate these data were about 10 hours. For each of the two sets of networks, a number of MLPNNs' architectures have been developed and tested. At this purpose, the following backpropagation learning rules: *i*) Conjugate Gradient backpropagation with Powell-Beale restarts (CGPB), *ii*) One Step Secant backpropagation (OSS), *iii*) Resilient backpropagation (RB), have been employed in conjunction with the modified Elliot sigmoid transfer functions (see [21] and references within). All the relevant information about the numerical experiments carried out, are summarized in Table 2, for the circular case and in Table 3, for the rectangular case. To improve the performances of neural computations

Table 2. Architectures, training algorithms and performances of MLPNNs' models of a lossy SIW circular resonator (all the times are in seconds).

Net	Neurons and Hidden Layers	Training Algor.	Epochs	GPU Time	GPU Time	RMSE
#C1	18, 24, 24, 18, 6	CGBP	202	5.28	11.02	$1.31 \cdot 10^{-4}$
#C2	18, 24, 24, 18, 6	OSS	157	4.95	12.10	$4.42 \cdot 10^{-4}$
#C3	18, 24, 24, 18, 6	RB	164	2.07	2.49	$2.81 \cdot 10^{-4}$
#C4	12, 24, 24, 12	CGBP	88	2.58	4.57	$6.72 \cdot 10^{-3}$
#C5	12, 24, 24, 12	OSS	170	4.46	9.90	$5.53 \cdot 10^{-3}$
#C6	12, 24, 24, 12	RB	175	1.85	2.12	$5.12 \cdot 10^{-3}$
#C7	24, 48, 24	CGBP	137	3.47	8.22	$7.84 \cdot 10^{-3}$
#C8	24, 28, 24	OSS	51	2.12	4.22	$92.72 \cdot 10^{-3}$
#C9	24, 28, 24	RB	190	2.04	3.02	$2.73 \cdot 10^{-3}$

Table 3. Architectures, training algorithms and performances of MLPNNs' models of a lossy SIW rectangular resonator (all the times are in seconds).

Net	Neurons and Hidden Layers	Training Algor.	Epochs	GPU Time	GPU Time	RMSE
#R1	13, 19, 29, 13, 7	CGBP	222	5.12	14.27	$1.23 \cdot 10^{-4}$
#R2	13, 29, 29, 13, 7	OSS	129	3.99	11.61	$6.11 \cdot 10^{-4}$
#R3	13, 29, 29, 13, 7	RB	109	1.58	2.10	$2.53 \cdot 10^{-4}$
#R4	11, 27, 27, 11	CGBP	149	3.51	7.46	$5.62 \cdot 10^{-3}$
#R5	11, 27, 27, 11	OSS	141	3.93	9.55	$20.01 \cdot 10^{-3}$
#R6	11, 27, 27, 11	RB	152	1.72	1.97	$6.73 \cdot 10^{-3}$
#R7	11, 27, 13	CGBP	145	2.93	4.49	$9.94 \cdot 10^{-3}$
#R8	11, 27, 13	OSS	169	3.81	7.41	$8.12 \cdot 10^{-3}$
#R9	11, 27, 13	RB	117	1.38	1.92	$1.72 \cdot 10^{-3}$

on GPU, data have been conveniently normalized and processed so that them were aligned properly in the GPU memory. In this way the MLPNN's training phase was about twice times faster than compared to the case of unprocessed data. As expected, and as it is confirmed by numerical results reported in Tables 2 and 3, using the GPU a reduction of the computational time is obtained in correspondence of

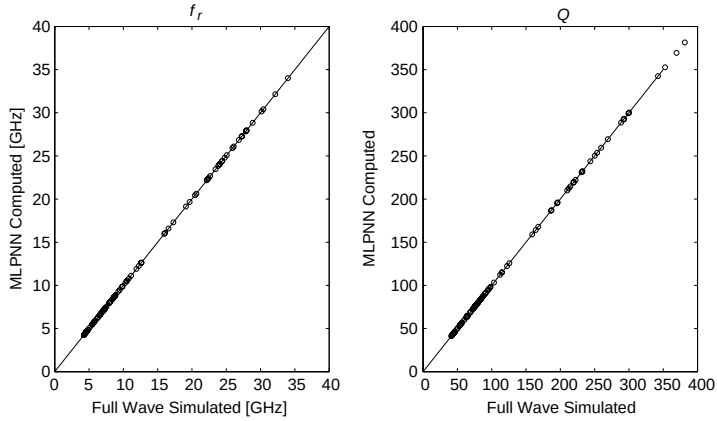

Figure 2. Scatter plots of the #C1 estimated and full wave computed resonant frequency f_r and Q factor, in the case of lossy SIW circular resonator.

Table 4. Resonant frequency and Q for a lossy circular SIW resonator ($R = 7\,\text{mm}$, $p = 2.2\,\text{mm}$, $\epsilon_r = 3.5$, $\tan(\delta) = 0.0035$, $h = 0.5\,\text{mm}$, $a_0 = 0.4$) computed by HFSS and estimated by #C1 network.

	Resonant Frequency f_r	Quality Factor Q
HFSS	8.965 GHz	188.38
MLPNN #C1	8.955 GHz	187.85

an increase of the number of MLPNN's neurons and hidden layers. At the same time an improvement of the RMSE, and consequently of the performances of the MLPNN model, can be also noticed. In term of this parameter, the best results have been obtained using the CGPB algorithm, while the RB is the faster. Figure 2 shown the scatter plots, provided by the best MLPNN architecture for the circular case (the MLPNN #C1), obtained comparing among them the values of f_r and Q obtained by full wave simulations and by MLPNN estimations. The tight grouping of these values along the diagonal axis gives an excellent indication of the ability of the network to capture the input-output relationship present in the data. Finally, two lossy SIW resonator have been implemented in the HFSS framework, and the resonant frequencies and the Q factors have been evaluated. Tables 4 and 5 shown the comparison between these results and those obtained by means of the networks #C1 and #R1. The excellent agreement

Table 5. Resonant frequency and Q for a lossy rectangular SIW resonator ($L = 24\,\text{mm}$, $W = 14\,\text{mm}$, $p = 2\,\text{mm}$, $\epsilon_r = 3.5$, $\tan(\delta) = 0.0035$, $h = 0.5\,\text{mm}$, $a_0 = 0.4$) computed by HFSS and estimated by #R1 network.

	Resonant Frequency f_r	Quality Factor Q
HFSS	6.710 GHz	191.65
MLPNN #R1	6.750 GHz	189.85

obtained confirms the capability of the MLPNN model to give an accurate evaluation of the couple f_r and Q over the whole range of the geometrical and electrical parameters considered for its training, in a time about thirty times shorter than a single full wave simulation.

6. CONCLUSIONS

In this paper, an effective approach to model the behavior of lossy SIW resonators, based on MLPNNs on GPU, is presented. Numerical results are consistent with full wave computations, confirming the robustness of the proposed approach. Once that the MLPNN model is trained, it can predict the fundamental resonant frequency f_r and the quality factor Q of an assigned lossy SIW resonator in a very fast and accurate way. Future investigations are aimed at the integration of this model in the framework of an automated high speed design procedure of microwave SIW devices on GPU. In fact a MLPNN provides a fast parametric model of a generic SIW structure, allowing to avoid the long full wave simulations times when evaluating changes in the layout geometry or substrate's parameters [23].

REFERENCES

1. Zhang, Q.-L., W.-Y. Yin, S. He, and L.-S. Wu, "Evanescent-mode substrate integrated waveguide (SIW) filters implemented with complementary split ring resonators," *Progress In Electromagnetics Research*, Vol. 111, 419–432, 2011.
2. Amendola, G., E. Arnieri, L. Boccia, and V. Ziegler, "Annular ring slot radiating element for integrated millimeter wave arrays," *Proceedings of 6th European Conference on Antennas and Propagation, EuCAP 2012*, 3082–3085, Prague, Czech Republic, 2012.
3. Boccia, L., A. Emanuele, E. Arnieri, A. Shamsafar, and G. Amendola, "Substrate integrated power combiners," *Proceedings of*

6th European Conference on Antennas and Propagation, EuCAP 2012, 3631–3634, Prague, Czech Republic, 2012.

4. Russo, I., L. Boccia, G. Amendola, and H. Schumacher, "Compact hybrid coaxial architecture for 3 GHz–10 GHz UBW quasi-optical power combiners," *Progress In Electromagnetics Research*, Vol. 122, 77–92, 2012.
5. HFSS Ansys, Ansys, 2013.
6. Abaei, E., E. Mehrshahi, G. Amendola,, E. Arnieri, and A. Shamsafar, "Two dimensional multi-port method for analysis of propagation characteristics of substrate integrated waveguide," *Progress In Electromagnetics Research C*, Vol. 29, 261–273, 2012.
7. Arnieri, E. and G. Amendola, "Analysis of substrate integrated waveguide structure based on the parallel-plate waveguide Green's function," *IEEE Transactions on Microwave Theory and Techniques*, Vol. 56, 1615–1623, 2008.
8. Arnieri, E. and G. Amendola, "Method of moment analysis of slotted substrate integrated waveguide arrays," *IEEE Transactions on Antennas and Propagation*, Vol. 59, 1148–1154, 2011.
9. Amendola, G., E. Arnieri, and L. Boccia, "Analysis of lossy SIW structures based on the parallel plates waveguide Green's function," *Progress In Electromagnetics Research C*, Vol. 33, 157–159, 2012.
10. Amendola, G., G. Angiulli, E. Arnieri, and L. Boccia, "Resonant frequencies of circular substrate integrated resonators," *IEEE Microwave and Wireless Components Letters*, Vol. 18, No. 4, 239–241, 2008.
11. Angiulli, G., E. Arnieri, D. De Carlo, and G. Amendola, "Fast nonlinear eigenvalues analysis of arbitrarily shaped substrate integrated waveguide (SIW) resonators," *IEEE Transactions on Magnetics*, Vol. 45, No. 3, 1412–1415, 2009.
12. Amendola, G., G. Angiulli, E. Arnieri, and L. Boccia, "Computation of the resonant frequency and quality factor of lossy substrate integrated waveguide resonators by method of moments," *Progress In Electromagnetics Research Letters*, Vol. 40, 107–117, 2013.
13. Humayun, K., L. Zhang, M. Yu, P. H. Aaen, J. Wood, and Q.-J. Zhang, "Smart modeling of microwave devices," *IEEE Microwave Magazine*, Vol. 11, 105–118, 2010.
14. Angiulli, G., D. De Carlo, G. Amendola, E. Arnieri, and S. Costanzo, "Support vector regression machines to evaluate resonant frequency of elliptic substrate integrate waveguide

resonators," *Progress In Electromagnetics Research*, Vol. 83, 107–118, 2008.

15. Luo, M. and K.-M. Huang, "Prediction of the electromagnetic field in metallic enclosures using artificial neural networks," *Progress In Electromagnetics Research*, Vol. 116, 171–184, 2011.
16. Wefky, A., F. Espinosa, L. D. Santiago, A. Gardel, P. Revenga, and M. Martinez, "Modeling radiated electromagnetic emissions of electric motorcycles in terms of driving profile using MLP neural networks," *Progress In Electromagnetics Research*, Vol. 137, 741–758, 2013.
17. Scanzio, S., S. Cumani, R. Gemello, F. Mana, and P. Laface, "Parallel implementation of artificial neural network training," *IEEE International Conference on Acoustics Speech and Signal Processing (ICASSP 2010)*, 4902–4905, 2010.
18. Pendlebury, J., "Artificial neural network simulation on CUDA," *IEEE/ACM 16th International Symposium on Distributed Simulation and Real Time Applications*, 228–233, 2012.
19. Angiulli, G., "On the computation of nonlinear eigenvalues in electromagnetics problems," *Journal of Electromagnetic Waves and Applications*, Vol. 21, No. 4, 527–532, 2007.
20. Hwu, W.-M., Ed., *GPU Computing Gems: Jade Edition*, Morgan Kaufmann, 2011.
21. Hu, H. Y. and J. Hwang, Eds., *Handbook of Neural Network Signal Processing*, CRC Press, 2010.
22. Sanders, J. and E. Kandrot, *CUDA by Example — An Introduction to General-purpose GPU Programming*, Addison-Wesley, 2011.
23. Angiulli, G., "Design of square substrate waveguide cavity resonators: Compensation of modelling errors by support vector regression machines," *American Journal of Applied Sciences*, Vol. 9, No. 11, 1872–1875, 2012.